In-Lab Drone's Attitude Maneuvering Fluency Evaluation by a Gyroscopic Lurch Index

SIMONE FIORI
Università Politecnica delle Marche
Dept. of Information Engineering
Via Brecce Bianche, 60131 Ancona
ITALY
s.fiori@univpm.it

NICOLA SABINO
Università Politecnica delle Marche
School of Informatics & Automation
Via Brecce Bianche, 60131 Ancona
ITALY
nicola.sabino94@gmail.com

ANDREA BONCI
Università Politecnica delle Marche
Dept. of Information Engineering
Via Brecce Bianche, 60131 Ancona
ITALY
a.bonci@univpm.it

Abstract: The present paper reports on the current progress about the laboratory-based assessment of the fluency of attitude maneuvering of a quadcopter. The manuscript illustrates a laboratory-based data-acquisition setup and a mathematical data-processing algorithm to test a novel attitude maneuvering fluency estimation index termed *geometric lurch*. The geometric lurch index is defined in terms of angular variables' values as returned by gyroscopic sensors that a quadcopter vehicles are equipped with. The results of several numerical tests, conducted on both synthetic and real-world gyroscopic signals, show that the geometric lurch index is fairly sensitive to the fluency of attitude maneuvering.

Key–Words: Attitude Maneuvering; Drone; Gyroscopic lurch; Inertial measurement unit; Quadcopter.

1 Introduction

A unmanned aerial vehicle is typically intended to be used as a search and rescue field robot as it allows for high levels of maneuverability, including the ability to hover. The unmanned aerial vehicle is able to acquire and to transmit data to an operator situated at a safe vantage point [6]. The structure of a quad-rotor helicopter, hereafter a *quadcopter* comprises four rotors attached at the ends of a symmetric light structure (see, e.g., the Figure 1). The key features of a

Figure 1: A Parrot AR Drone Quadricopter, 2.0 Elite Edition.

quadcopter structure are *rigidity* and *symmetry* [6]. To avoid unstable flight phenomena and to improve ma-neuverability, the structure should be as rigid as possible, while maintaining the lightest possible weight. Symmetry is also of great importance, namely, the center of gravity should be kept as close to the middle of the drone as possible, so as to facilitate the control of the vehicle. Likewise a conventional helicopter, a quadcopter is a six degree-of-freedom, highly non-linear, multi-variable, strongly coupled, and under-actuated system [6].

The availability of inexpensive commercial sensors to measure kinematic variables, such as position, speed and orientation, boosted the design of small flying objects controlled by a remote side by a human operator or by an automated control system.

In particular, in order to measure the orientation (or *attitude*) of a non-moving object (yaw, pitch and roll), a three-axis accelerometer may be employed. For a *static* vehicle, a three-axis accelerometer returns the value of the gravity field on three axes and, therefore, its orientation. In fact, since the gravitational force always points toward the center of the earth, we can know how the accelerometer device, and hence the vehicle, is tilted. Such method has been used in smartphones and may provide accurate results. However, if a vehicle or a smartphone starts translating in space, it becomes subjected to an additional force that changes its acceleration: The assumption that was made previously to compute its orientation will not be valid anymore, hence the calculated orientation will not be correct any longer.

The most common used sensor in quadcopter control is the *gyroscopic* sensor. A gyroscope returns the angular velocity around three axes of space in degrees per seconds the actual attitude may be computed by appropriate numerical techniques. A problem in quadcopter's data acquisition and control is the sensitivity of sensors to vibrations and shocks due to the nature of the sensors, in particular:

○ As mentioned, a gyroscope is only able to measure an angular rate, not an absolute orientation. Any numerical integration method to compute the actual attitude over a vehicle will unavoidably emphasize the contribution of the noise and of the vibrations/shocks in the measurements.

○ All the common gyroscopes show a *drift*, which implies that even if a drone flies steady or do not move at all, the sensor will output nonzero angular velocities. Depending on the quality of the sensor, the drift can be pretty big for some sensors (e.g., it can go up to 2 degrees per second on a commercial gyroscope), therefore destroying the accuracy of the measurement when such readouts get numerically integrated to compute the actual attitude of the vehicle.

Practitioners know different ways of getting the most accurate orientation estimate from a combination of sensors. The most common approach is a *complementary filter*. The idea behind the complementary filter is that the filtered accelerometer value of the angle is not subject to drift, therefore it may be used to correct the readouts by the gyroscope. The same complementary filter may be exploited when the above-mentioned sensors are used in conjunction with a magnetic compass (which returns the local direction of the earth's magnetic field), to compute the attitude of the quadcopter. Another well-known method to filter out the artifacts from the sensed data is to pre-process the acquired measurements through a Kalman filter [7].

Most research studies in aerial vehicles control focus on the design of control strategies to ensure smooth maneuvering of drones [8]. However, unpredictable events, such as the drone being shoved by a strong gust of wind or being hit by another flying object, might make an attitude maneuver less smoother than predicted. The present paper focuses on the in-lab assessment of the *fluency* during maneuvering of a quadcopter vehicle by means of a mathematical algorithm that is able to emphasize the vibration and shocks measured by gyroscopic sensors during maneuvering.

The large amount of data arising from kinematic measurements call for a data-processing technique to evaluate the fluency during attitude maneuvering of a quadcopter. In particular, the present contribution

proposes and tests a novel kinematic index termed *gyroscopic lurch*. The gyroscopic lurch arises as a mathematical extension of the known concept of Cartesian kinematic lurch, that is, of the time-derivative of the acceleration of a trajectory on a Cartesian (flat) space. The contribution [5] surveys several applications of Cartesian lurch, namely, high dynamic motion aerial vehicle trace measurement, earthquake-resistant structures design, analysis of mechanisms of high-speed automatic control of machines, study of human responses in high-speed moving vehicle.

The current manuscript aims primarily at proposing a mathematical algorithm to compute a numerical index that could work as a synthetic indicator of the fluency of attitude maneuvering and at illustrating a possible in-lab test-bed to conduct experiments on its numerical features. The current manuscript presents a preliminary study on the notion of *geometric lurch* and on its physical measurement and calculation. Possible real-world applications that are currently under investigation will be discussed in the concluding Section.

The current paper is organized as follows. The Section 2 illustrates the in-lab data-acquisition setup and recalls some fundamental notions from the mathematical theory of attitude maneuvering. The Section 3 defines the geometric lurch index in terms of angular variables sensed by gyroscopes that aerial vehicles are supposed to be equipped with. The Section 4 illustrates the results of numerical experiments, conducted on both synthetic and real-world, acquired data, about the estimation of the fluency of attitude maneuvering. The Section 5 concludes the paper.

2 In-lab acquisition of gyroscopic data

The Subsection 2.1 illustrates the laboratory setup used to acquire gyroscopic data from a quadcopter, while the Subsection 2.2 recalls some fundamental notions and properties from the mathematical theory of attitude maneuvering.

2.1 Data acquisition setup

The gyroscopic data that represent the instantaneous orientation of a quadcopter were collected in a laboratory through an Inertial Measurement Unit (IMU, see Figure 2) mounted on the drone, as a part of a typical setup for robot control [1].

The inertial measurement unit was selected as a MPU-6050 integrated 6-axis Motion-Tracking device that combines a 3-axis gyroscope and a 3-axis accelerometer [4]. The MPU-6050 device con-
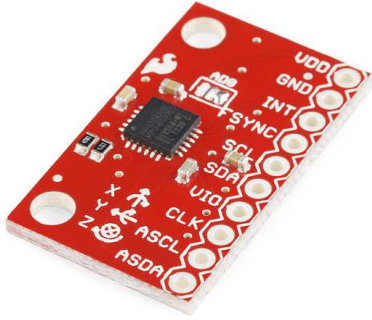
Figure 2: A *SparkFun Electronics*, triple axis accelerometer and gyroscope (model MPU-6050). The depicted IMU includes a gyroscope that measures the orientation with respect to a fixed reference frame.

Figure 3: An ARDUINO[TM] Uno board. The digital input channels to connect to the IMU and the Universal Serial Bus (USB) port to connect the ARDUINO[TM] micro-controller board to a PC can be clearly seen.

sists of three independent vibratory MEMS[1] gyroscopes, which detect rotation about the $X-$, $Y-$, and $Z-$axes. When the gyroscopes are rotated about any of the sense axes, the Coriolis effect causes a vibration that is detected by a capacitive pickoff. The resulting signal is amplified, demodulated and filtered to produce a voltage signal that is proportional to the angular rate. Such voltage is digitized using individual on-chip 16-bit analog-to-digital converters to sample each axis. The full-scale range of the gyroscopic sensors may be digitally programmed to ± 250, ± 500, ± 1000 or ± 2000 degrees per second. The analog-to-digital converters sample rate is programmable from 8000 samples per second to 3.9 samples per second, and user-selectable low-pass filters enable a wide range of cut-off frequencies.

The IMU interfaces with an ARDUINO[TM] Uno micro-controller board trough an Inter Integrated Circuit (I^2C) bus, while the ARDUINO[TM] board interfaces with a personal computer (PC) through a serial USB cable. The ARDUINO[TM] is a standalone general purpose micro-controller used as interface to low-voltage electronic components, electro-mechanical components and electronic systems like personal computers, modems and wireless devices. The ARDUINO[TM] Uno board is displayed in the Figure 3. The libraries used to pilot the MPU-6050 inertial measurement unit via an I^2C bus and to acquire the gyroscopic data in an appropriate format were written by Jeff Rowberg (http://www.sectorfej.net/)

---

[1]The acronym *MEMS* stands for micro-electro-mechanical system. MEMS usually consist of a central unit that processes data and a number of components that interact with the surroundings such as the microsensors [9].
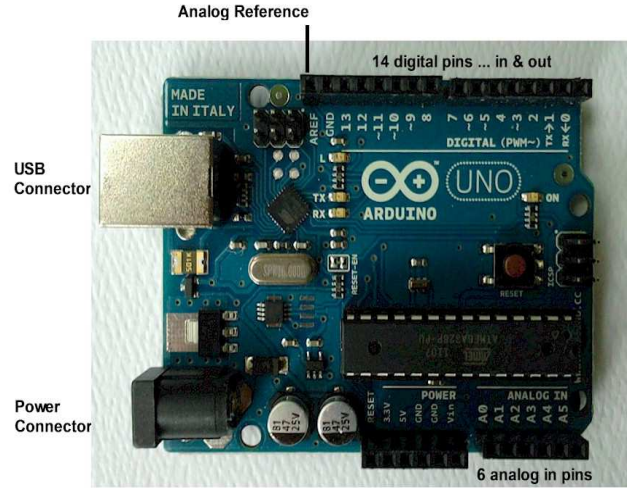
and are publicly available at https://github.com/jrowberg/i2cdevlib/tree/master/Arduino/MPU6050.

The MATLAB[®] computing platform was used to acquire the signals from the IMU and to execute the data-processing algorithm of interest on the acquired signals. The MATLAB[®] treats a port like a file, therefore, reading out the signals from the IMU via the ARDUINO[TM] board may be performed like reading the records of a data-file, as shown in the code excerpt Listing 1. In this example, the PC was running a Linux OS and the ARDUINO[TM] was supposed to connect to the USB port labeled 'USB4'.

The gyroscopic signals were acquired under the form of a sequence of 3 angles $(\psi_k, \theta_k, \phi_k)$, with $k = 1, \ldots, N$, termed, respectively, *yaw*, *pitch* and *roll*, as exemplified in the Figure 4. An example of acquired angular data is shown in the Figure 5.

2.2 From the yaw-pitch-roll representation to the angular velocity vector

Let us denote again by ψ the yaw angle, by θ the pitch angle and by ϕ the roll angle. Such variables represent the orientation of the drone with respect to a laboratory's inertial reference system. The rotation matrix R corresponding to a triple (ψ, θ, ϕ) may be written as:

$$R = R_z(\phi)R_y(\theta)R_x(\psi), \qquad (1)$$

where the functions R_x, R_y and R_z denote standard rotation functions about the canonical axes [6]. During an attitude maneuver, the angles (ψ, θ, ϕ) change

Listing 1: MATLAB® script to acquire the gyroscopic signals from the IMU via the ARDUINO™ board.

```
% Script to read out IMU signals by the
% MATLAB computing platform
% Version: May 2015
% The transfer rate is of 115200 baud

% Initializes the serial port
arduino=serial('/dev/ttyUSB4');
set(arduino,'baudrate',115200)
fopen(arduino);
% Data matrix
N = 4000; % 4000 readouts
data = zeros(3,N);
% Data acquisition
for i = 1:N,
 data(:,i) = fscanf(arduino,'%f');
 % Float-type data
end
% Saves the acquired data
save data;
```

with time and the rate of change of orientation of the drone varies according to the law

$$\dot{R} = \frac{d}{dt} R_z(\phi(t)) R_y(\theta(t)) R_x(\psi(t)). \qquad (2)$$

From the theory of 3D rotations, it is known that such change rate obeys the rule $\dot{R} = R\Omega$, where the matrix Ω is termed *angular velocity matrix* and is skew-symmetric, namely, of the form

$$\Omega(t) = \begin{bmatrix} 0 & \omega_1(t) & \omega_2(t) \\ -\omega_1(t) & 0 & \omega_3(t) \\ -\omega_2(t) & -\omega_3(t) & 0 \end{bmatrix}. \qquad (3)$$

The independent components of the angular velocity matrix may be computed by the inverse relationship $\Omega = R^T \dot{R}$ and were found to relate to the rate of change of the yaw-pitch-roll angular coordinates by

$$\begin{bmatrix} \omega_1 \\ \omega_2 \\ \omega_3 \end{bmatrix} = \begin{bmatrix} -\cos(\phi)\cos(\theta) & \sin(\phi) & 0 \\ \cos(\theta)\sin(\phi) & \cos(\phi) & 0 \\ \sin(\theta) & 0 & -1 \end{bmatrix} \begin{bmatrix} \dot{\psi} \\ \dot{\theta} \\ \dot{\phi} \end{bmatrix}. \qquad (4)$$

The angular velocities ω_1, ω_2 and ω_3 are the Cartesian coordinates of the angular velocity vector denoted as ω.

3 Gyroscopic lurch index

The Subection 3.1 defines the geometric lurch index in terms of angular variables sensed by gyroscopes ,
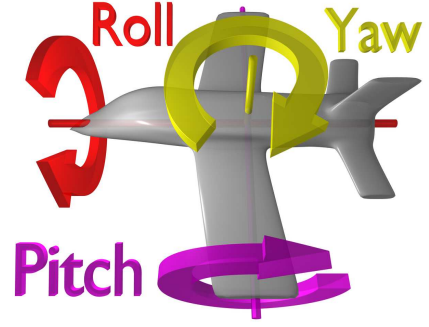

Figure 4: Physical meaning and pictorial illustration of the yaw, pitch and roll angles to describe the instantaneous orientation of a flying device.
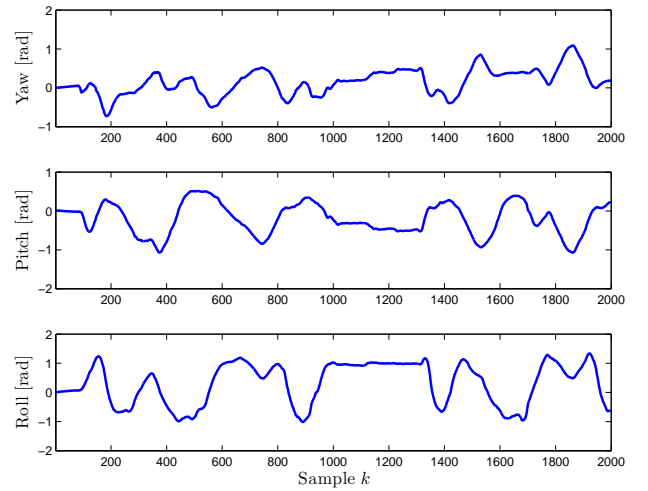

Figure 5: Exemplary gyroscopic data acquired by an IMU driven by an ARDUINO™ board. Graphical representation of the three angles yaw, pitch and roll. Only the first 2,000 samples are shown for the sake of clarity.

while Subsection 3.2 presents a comparison between the proposed geometric kinematic lurch index and the known Cartesian kinematic lurch index.

3.1 Definition of gyroscopic lurch index

The kinematic state of a moving rigid object may be represented by the position of its center of mass and by a three-dimensional vector that describes its instantaneous rotation speed, termed *angular velocity*, denoted by $\omega \in \mathbb{R}^3$. In the present research endeavor, we focus on the evaluation of the rotational fluency of a quadcopter during attitude maneuvering. The direction of the vector ω represents the orientation of the rotation axis of the rigid object and its amplitude represents the actual rotation speed.

In terms of gyroscopic data only, the motion of a quadcopter may be described by a continuous-time signal $\omega(t) \in \mathbb{R}^3$ that represents the instantaneous rotation speed and orientation of the drone over time. The vector-field ω is a tangent vector-field in the trivialized tangent bundle of the Lie group of three-dimensional rotations and, as such, obeys to the rules of calculus prescribed by differential geometry, upon metrization of the tangent bundle. The manuscript [10] describes the mathematical structure of such space and related calculations in details. The calculations are based on the notion of *covariant derivative* ∇ of a vector field along a vector field.

In order to evaluate the fluency of the rotational motion of a quadcopter, in robotics a specific vector field is calculated that is the *lurch* associated to a velocity field. The lurch is defined as the second time-derivative of the speed (namely, as the derivative of the acceleration). In the present study, therefore, we define the lurch associated with the field ω as *gyroscopic lurch*. According to the calculations explained in [10], while the instantaneous acceleration associated to a field ω is simply $\nabla_\omega \omega = \dot{\omega}$, its second-order time-derivative takes on the form [10, Proposition 4.2]:

$$\nabla_\omega^2 \omega = \ddot{\omega} + \tfrac{1}{2}\omega \times \dot{\omega}, \quad (5)$$

where the symbol $\times$ denotes the standard three-dimensional vector cross product. The scalar gyroscopic lurch is the amplitude of the second-covariant derivative (5), namely $\|\nabla_\omega^2 \omega\|$.

If we denote by $[0,\ T]$ the time interval that the gyroscopic data measurement was taken over, an index of attitude maneuvering fluency may be defined as the time-integral of the scalar gyroscopic lurch by:

$$L = C_L \int_0^T \left\| \ddot{\omega}(t) + \tfrac{1}{2}\omega(t) \times \dot{\omega}(t) \right\| dt, \quad (6)$$

where the constant C_L needs to be defined in a way that makes the index (6) independent of the maneuvering time and of the maneuvering speed, in order to enable a user to compare different values of the index (6) pertaining to different quadcopter trajectories.

In order to define such a scaling constant, we define first the accumulated angular speed as

$$S = \int_0^T \|\omega(t)\| dt, \quad (7)$$

and the normalization constant as

$$C_L = \frac{T^2}{S}. \quad (8)$$

The computation of the gyroscopic lurch index starting from a Euler-angles data-sequence may be performed, in MATLAB® language, through the function in the Listing 2.

Listing 2: Function to compute the normalized gyroscopic lurch index (6.

```matlab
% MATLAB function to compute the
% gyroscopic lurch of an angular velocity
% data omega over a time-interval T
% Version: November 2015

function [S,L] = glurch(omega,T)
N = size(omega,2); DT = T/N;
S = DT*sum(sqrt(sum(omega.^2,1)));
omegap = diff(omega,1,2)/DT;
omegapp = diff(omegap,1,2)/DT;
gl = omegapp + 0.5*...
 cross(omega(:,1:N-2)',omegap(:,1:N-2)')';
L = (DT^2/S)*sum(sqrt(sum(gl.^2,1)));
```

3.2 Comparison with the Cartesian lurch

The gyroscopic lurch differs substantially from the popular Cartesian lurch used in applications [5]. Given an angular speed field ω, its second-order time-derivative may be defined *Cartesian lurch*. In particular, denoting the Cartesian coordinates of ω as

$$\omega(t) = [\omega_1(t)\ \omega_2(t)\ \omega_3(t)]^T, \quad (9)$$

the squared scalar Cartesian lurch computes as

$$\|\ddot{\omega}\|^2 = \ddot{\omega}_1^2 + \ddot{\omega}_2^2 + \ddot{\omega}_3^2. \quad (10)$$

Conversely, by using the Cartesian parametrization (9) in the formula to compute the squared scalar gyroscopic lurch, it is readily obtained that:

$$
\begin{aligned}
\|\nabla_\omega^2 \omega\|^2 &= \left(\ddot{\omega}_3 + \frac{\omega_1 \dot{\omega}_2}{2} - \frac{\omega_2 \dot{\omega}_1}{2} \right)^2 \\
&+ \left(\ddot{\omega}_2 - \frac{\omega_1 \dot{\omega}_3}{2} + \frac{\omega_3 \dot{\omega}_1}{2} \right)^2 \\
&+ \left(\ddot{\omega}_1 + \frac{\omega_2 \dot{\omega}_3}{2} - \frac{\omega_3 \dot{\omega}_2}{2} \right)^2. \quad (11)
\end{aligned}
$$

Apparently, the scalar gyroscopic lurch differs greatly from the scalar Cartesian lurch. For example, if in a point of a trajectory the Cartesian lurch is negligible, namely $\ddot{\omega}_1^2 + \ddot{\omega}_2^2 + \ddot{\omega}_3^2 \approx 0$, still the gyroscopic lurch may differ considerably from zero, because its squared value would approximately equal $\frac{1}{4}[(\omega_1\dot{\omega}_2 - \omega_2\dot{\omega}_1)^2 + (\omega_2\dot{\omega}_3 - \omega_3\dot{\omega}_2)^2 + (\omega_1\dot{\omega}_3 - \omega_3\dot{\omega}_1)^2]$.

4 Numerical assessments

The first experiment pertains to synthetic data, generated by means of a specific numerical algorithm, and

was meant to evaluate the sensitivity of the gyroscopic lurch index L (6) with respect to the known smoothness of a rotational signal. The second set of experiments pertain to acquired data measured in different conditions.

4.1 Numerical assessment of synthetic data

In order to simulate the change of orientation of a quadcopter during attitude maneuvering, a pseudo-random data generator, especially developed to simulate a fluent maneuvering and an erratic maneuvering mode, was made use of.

In particular, two data sets were synthetically generated by gluing together five sub-data-streams. Each sub-stream is of the type fluent (F) and erratic (E). The F-type sub-stream was generated through the a formula described in [10], while the E-type sub-stream was generated via an auto-regressive moving average ARMA(1,0) system over the Lie group SO(3) described in [2, 3].

A number $N = 800$ of samples were generated for each data-set: The first synthetic gyroscopic dataset was made up as the sequence 'FFFFF' of substreams, while the second data-set was made up as the sequence 'FEFEF' of sub-streams. The orientation angles corresponding to the two obtained gyroscopic data are displayed in the Figure 6. It is interesting to
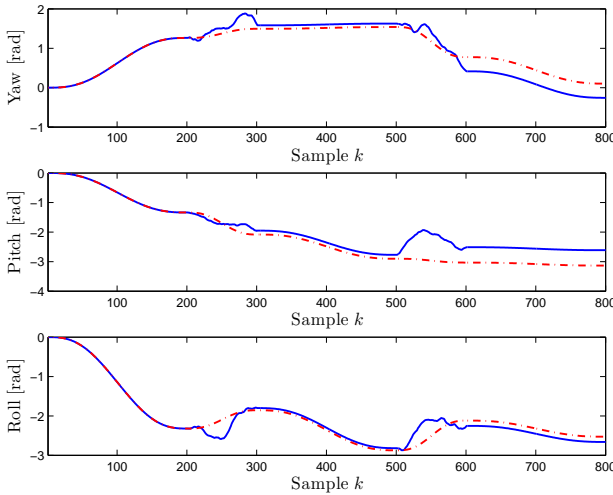

Figure 6: Synthetic gyroscopic data. Graphical representation of the angles generated synthetically. (Dot-dashed line: Fluent attitude maneuvering mode 'FFFFF'. Solid line: Erratic attitude maneuvering mode 'FEFEF'.)

note that the synthetic gyroscopic data illustrated in the Figure 6, namely a fluent maneuver and an erratic maneuver are supposed to be the same except for a

few shocks in the erratic attitude maneuvering, however, the two curves in each panel tend to diverge in time due to a (simulated) drift in the sensors.

The Figure 7 illustrates the physical meaning of a gyroscopic data by simulating the rotation of a rigid body according to the erratic signal. As it is readily appreciated, in some time-intervals the rigid object moves smoothly taking nearly similar orientations, while in some time-intervals the object's orientation varies abruptly.
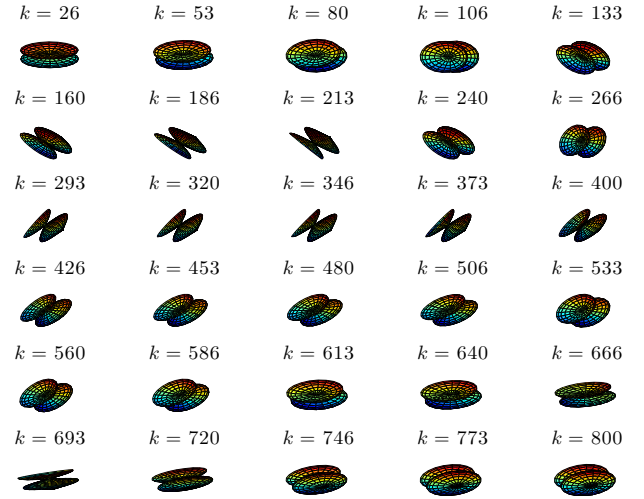

Figure 7: Synthetic gyroscopic data. Graphical representation of the result of the non-smooth rotation signal on a solid shape (downsampled for clarity).

The results of the numerical evaluation of the accumulated angular speed S and of the gyroscopic lurch index L pertaining to such synthetic data are displayed in the Table 1. The obtained numerical results suggest that the gyroscopic lurch index is very sensitive to the attitude maneuvering fluency conveyed by gyroscopic data.

	Cumul. ang. speed	Lurch
Fluent	0.8691	0.8552
Erratic	1.2432	286.3964

Table 1: Indexes calculated on two synthetic gyroscopic data.

4.2 Numerical assessment of acquired quadcopter data

The acquired gyroscopic data are referred to a number of experiments on different attitude maneuvering strategies operated by the quadcopter shown in the Figure 8.

Figure 8: A quadcopter designed at the Department of Information Engineering of the Università Politecnica delle Marche at Ancona (Italy).

A first set of data is shown in the following Figures. In particular, the data pertaining to the *Maneuver 1* are shown in the Figure 9, the data pertaining to the *Maneuver 2* are shown in the Figure 10, the d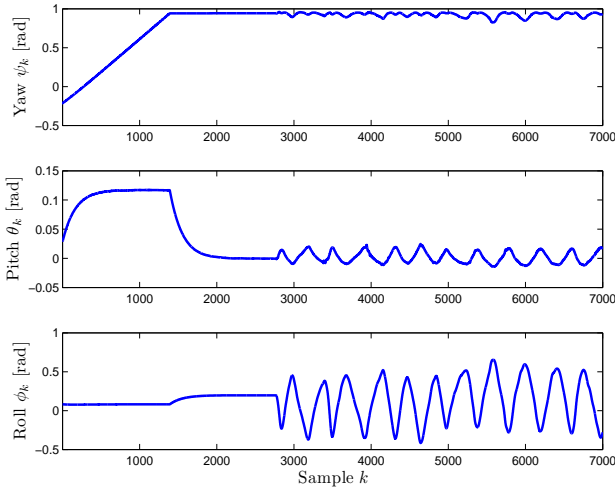ata pertaining to the *Maneuver 3* are shown in the Figure 11 and the data pertaining to the *Maneuver 4* are shown in the Figure 12.

Figure 9: First real-world data-set: Acquired gyroscopic data referred to the *Maneuver 1*.

The data were acquired with a sampling period of about 10ms. From the Figures, it is immediate to recognize that the first 2000 samples, approximately, do not carry any information about the vehicle orientation as the corresponding signal portion is due to the self-setup and calibration of the gyroscopic sensor. In the evaluation of the geometric lurch index, the first 2000 samples were, therefore, discarded.

The results of the numerical evaluation of the accumulated angular speed S and of the gyroscopic lurch index L pertaining to such real-world data are
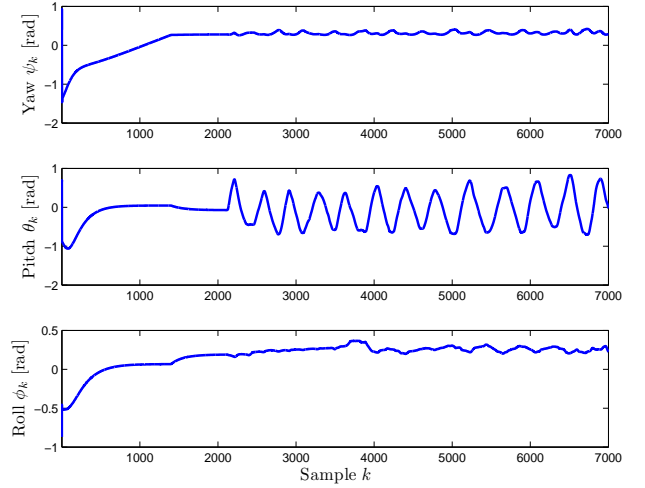

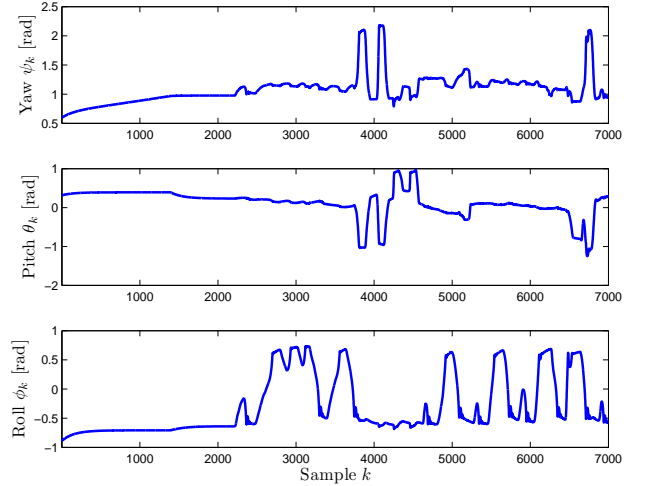Figure 10: First real-world data-set: Acquired gyroscopic data referred to the *Maneuver 2*.

Figure 11: First real-world data-set: Acquired gyroscopic data referred to the *Maneuver 3*.

summarized in the Table 2. The obtained numerical results confirm that the gyroscopic lurch is fairly sensitive to the attitude maneuvering fluency conveyed by the acquired gyroscopic data. In particular, according to the fluency ranking induced by the geometric lurch index, the *Maneuver 2* is substantially more fluent compared to the *Maneuvers 1, 3* and *4*. It is interesting to compare the values of the *Cumulative lurch* versus the value of the *Cumulative distance* for the four maneuvers, where the above indexes are defined as:

$$\text{Cumulative distance at time } t =$$
$$\int_0^t \|\omega(t)\| dt, \tag{12}$$
$$\text{Cumulative lurch at time } t =$$
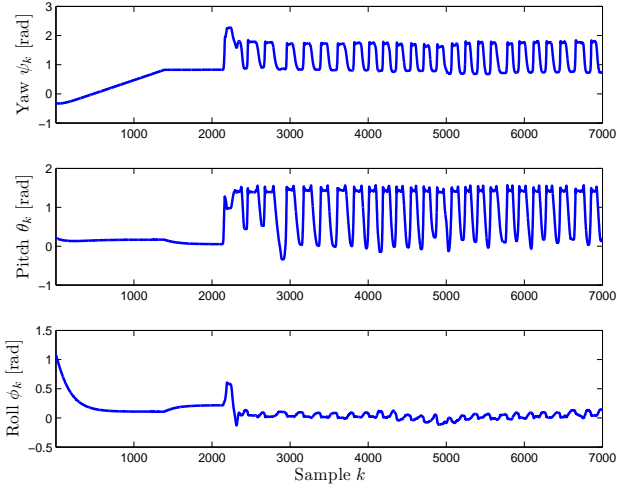$$T^2 \int_0^t \|\nabla_{\omega(t)}\omega(t)\| dt. \tag{13}$$

Figure 12: First real-world data-set: Acquired gyroscopic data referred to the *Maneuver 4*.

	Cumul. ang. speed	Lurch
Maneuver 1	18.59	12.09
Maneuver 2	29.98	8.61
Maneuver 3	40.85	15.21
Maneuver 4	108.66	14.90

Table 2: Indexes calculated on four gyroscopic data-sets acquired in the laboratory.

The value of the Cumulative lurch versus the value of the Cumulative distance for the four maneuvers are illustrated in the Figure 13.

A second set of gyroscopic signals were acquired by simulating the actual flight of a quadcopter. The results of the numerical evaluation of the accumulated angular speed S and of the gyroscopic lurch index L pertaining to such real-world data sets are summarized in the Table 3. The obtained numerical results confirm that the gyroscopic lurch is fairly sensitive to the attitude maneuvering fluency conveyed by the acquired gyroscopic data. According to the fluency ranking in-

	Distance	Lurch index
Maneuver 1	3.23	60.48
Maneuver 2	2.79	80.11
Maneuver 3	4.69	49.64
Maneuver 4	6.28	36.67
Maneuver 5	6.98	34.19
Maneuver 6	8.24	30.01

Table 3: Indexes calculated on six gyroscopic data-sets acquired in the laboratory.

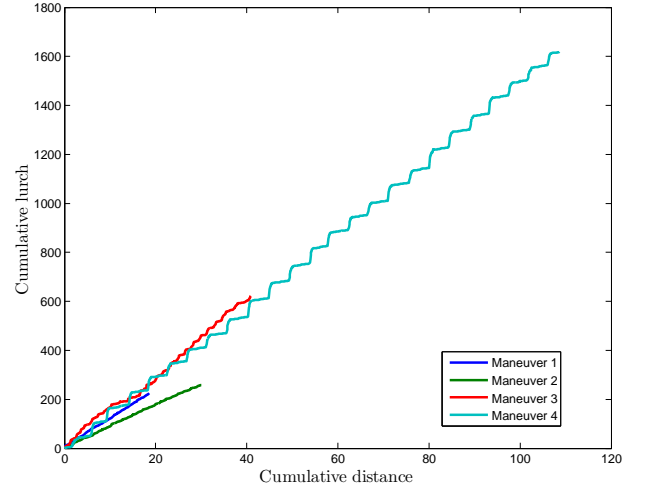duced by the geometric lurch index, the *Maneuver 6*,

Figure 13: First real-world data-set: Cumulative lurch versus Cumulative distance.

whose acquired gyroscopic signals are shown in the Figure 14, is the most fluent attitude maneuver in this data-set, while the *Maneuver 2*, whose acquired angular signals are shown in the Figure 15 is the most erratic one.
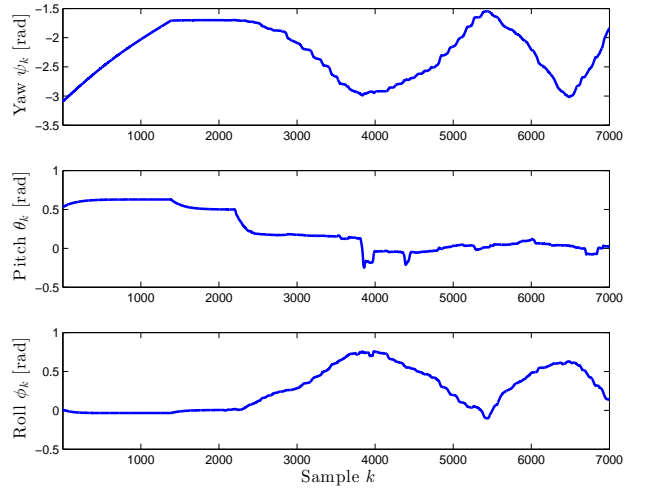

Figure 14: Second real-world data-set: Acquired gyroscopic data referred to the *Maneuver 6*.

The value of the Cumulative lurch versus the value of the Cumulative distance for the six maneuvers are illustrated in the Figure 16.

5   Conclusion

The present manuscript illustrates a laboratory-based data-acquisition setup and a mathematical data-processing algorithm to test a novel attitude maneuvering fluency estimation index termed geometric
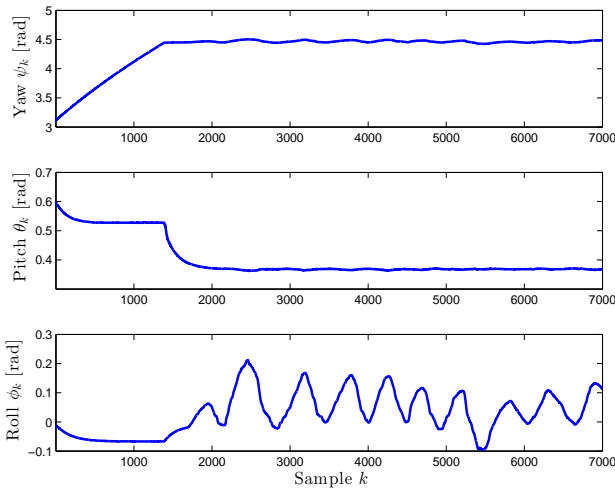
Figure 15: Second real-world data-set: Acquired gyroscopic data referred to the *Maneuver 2*.
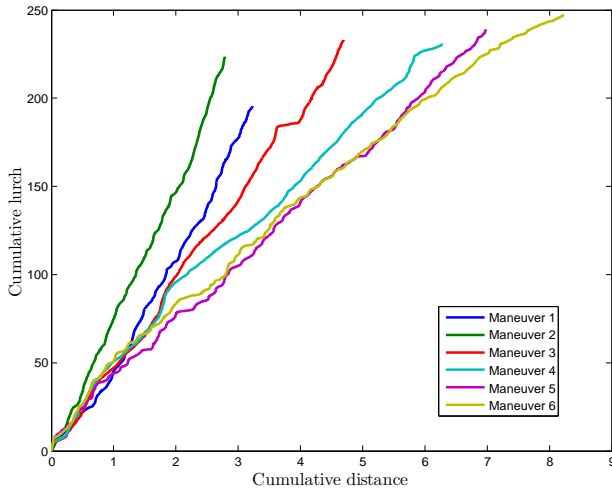

Figure 16: Second real-world data-set: Cumulative lurch versus Cumulative distance.

lurch. After recalling some fundamental notions from the mathematical theory of attitude maneuvering, we define the geometric lurch index in terms of angular variables' values are returned by gyroscopic sensors that quadcopter-type aerial vehicles are equipped with. The results of several numerical tests, conducted on both synthetic and real-world gyroscopic signals, show that the geometric lurch index is fairly sensitive to the fluency of attitude maneuvering.

The next steps of the present research will be to explore the sensitivity of the geometric lurch index in a series of outdoor tests by equipping the quadcopter with an acquisition system that is able to transmit the sensed gyroscopic data wirelessly to a remote personal computer in order to investigate on the usefulness of the lurch index in a real-time control problem.

Moreover, in order to adapt the proposed geometric lurch index to real-time processing, it will be necessary to reformulate the proposed method to compute the lurch index as a computationally-light, recursive, on-line algorithm.

Further research activities could be conducted about the investigation of the sensitivity of the lurch index on self-balanced autonomous ground vehicles instead of unmanned aerial vehicles. On these vehicles, the lurch index could be used for the inclination fluency estimation, to identify the sensitivity of sensors to vibrations and shocks due to the rough terrains.

References:

[1] A. Bonci, M. Pirani, M. Rossi and E.M. Gabbanini, Embedded system for a Ballbot robot, in *Proceedings of the 12th Workshop on Intelligent Solutions in Embedded Systems* (WISES'2015, October 29-30, 2015, Ancona – Italy). In press

[2] S. Fiori, Auto-regressive moving-average discrete-time dynamical systems and autocorrelation functions on real-valued Riemannian matrix manifolds, *Discrete and Continuous Dynamical Systems - Series B*, Vol. 19, No. 9, pp. 2785 – 2808, November 2014

[3] S. Fiori, Auto-regressive moving average models on complex-valued matrix Lie groups, *Circuits, Systems & Signal Processing*, Vol. 33, No. 8, pp. 2449 – 2473, 2014

[4] MPU-6000 and MPU-6050 Product Specification, Revision 3.4, August 2013

[5] Y. Xueshan, Q. Xiaozhai, G.C. Lee, M. Tong and C. Jinming, Jerk and jerk Sensor, in *Proceedings of the 14th World Conference on Earthquake Engineering* (Beijing, People's Republic of China), October 2008

[6] Y. Naidoo, R. Stopforth and G. Bright, Quadrotor unmanned aerial vehicle helicopter modelling & control, *International Journal of Advanced Robotic Systems*, Vol. 8, No. 4, 139 – 149, 2011

[7] G.G. Rigatos, Nonlinear Kalman Filters and Particle Filters for integrated navigation of unmanned aerial vehicles, *Robotics and Autonomous Systems*, Vol. 60, No. 7, pp. 978 – 995, July 2012

[8] S.L. Scrivener and R.C. Thompson, Survey of time-optimal attitude maneuvers, *Journal of Guidance, Control, and Dynamics*, Vol. 17, No. 2, pp. 225 – 233, 1994

[9] J.-B. Waldner, *Nanocomputers and Swarm Intelligence*, p. 205, John Wiley & Sons (London), April 2008

[10] M. Žefran and V. Kumar, Planning of smooth motions on SE(3), in *Proceedings of the 1996 IEEE International Conference on Robotics and Automation* (Minneapolis, MN, USA - April 1996), pp. 121 – 126, 1996